Security of Infocommunication Systems and Internet of Things

2023 Vol 1, No 1

https://doi.org/10.31861/sisiot2023.1.01007

Received 15 May 2023; revised 26 May 2023; accepted 12 June 2023; published 30 June 2023

Protecting IoT Wearable Devices from Electromagnetic Radiation Using Radio-Opaque Fabrics

Andriy Semenov*, Maksym Prytula, Oleksandr Stalchenko and Oleksandr Donskyi

Faculty of Information Electronic Systems, Vinnytsia National Technical University, Vinnytsia, Ukraine

*Corresponding author (E-mail: semenov.a.o@vntu.edu.ua)

ABSTRACT The number of sources of electromagnetic radiation is increasing every day. In most cases, electromagnetic radiation has a negative effect on the human body, animals, and other living beings. Electromagnetic radiation negatively affects the operation of electronic devices. Due to the electromagnetic radiation of electronic devices, information may leak from them. The negative impact of electromagnetic radiation on the human body provokes a high level of fatigue, headache, heartache, etc. The everyday use of mobile equipment, household magnetic appliances (for example, microwave ovens), and telecommunication networks puts the majority of the planet's population at risk. Otherwise, the external influence of electromagnetic fields on the various sensors used in the IoT can contribute to receiving incorrect data from the sensors. The powerful external influence of the electromagnetic field on devices that process large data sets can contribute to a failure in mathematical calculations. Thus, protection from electromagnetic fields is necessary not only for electronic devices but also for human protection. Radio-opaque fabrics are one of the modern materials for protection from electromagnetic radiation. They can be used to protect stationary objects and wearable IoT devices and to protect people. Industrial samples of foreign and Ukrainian radio-opaque fabrics were analyzed in the work. Ukrainian manufacturers continue to develop new variants of radio-opaque fabrics. The next options for radiopaque fabrics are fabrics G7, G8, and G9. The article proposed and described a method of researching the shielding properties of the fabric. Experimental studies were carried out, and the shielding coefficient was calculated in the frequency range of 50 MHz - 2 GHz for two fabrics G7 and G8. Experimental studies were carried out for two cases of the location of fabric fibers relative to the radiating antenna and field polarization. Plots of dependences of the shielding coefficient for two fabrics with different locations of fabric fibers were presented. A comparative analysis of the shielding coefficients of two fabrics was made, and relevant conclusions were presented.

KEYWORDS IoT, radio-opaque fabrics, shielding coefficient, frequency, electromagnetic field.

I. INTRODUCTION

Today, wearable communication devices that emit electromagnetic radiation are used in almost every sphere of activity. This is especially true for sensor networks and wearable IoT devices used in medical applications. As a result, the problem of protecting against information leakage through electromagnetic radiation and protecting these devices from external electromagnetic radiation is becoming more acute [1].

To address this problem, metal sheets, grids, and radio-opaque fabrics are used. Recently, radio-opaque fabrics have become more popular as they are more convenient to use. There are a number of foreign analogues of radio-opaque fabric [2, 3], but their use in Ukraine is limited primarily due to their high cost. Therefore, it is important to create Ukrainian analogues of radio-opaque fabric.

Currently, the first Ukrainian samples of radio-opaque fabric (Fabric 1 and Fabric 2) have been created. It is important to study the characteristics of the developed analogues of domestic radio-opaque fabrics. One of the modern approaches to screen implementation is the use of radio-opaque materials [1, 3]. Materials with a honeycomb structure, pyramidal or prickly surface possess the best properties with maximum absorption and minimum reflection [3]. Examples of modern radio-opaque materials are "Lebeda", "Lotos", and "Mokh" [4]. At present, the first radio-opaque fabrics of Ukrainian production N1, N2, and N3 have already been created. However, developers continue their work in this direction and propose new options for radio-opaque fabrics such as G7, G8, and G9. In this study, the authors have investigated the screening properties of G7 and G8 fabrics.

II. ANALYSIS OF THE IMPACT OF EXTERNAL ELECTROMAGNETIC FIELD

The speed of modern technical devices is constantly increasing, which is due to the increase in the operating frequencies of their individual components. This leads to a decrease in the interference protection of the devices from the influence of external electromagnetic fields. Therefore, when designing high-speed IoT systems, the significance of ensuring interference protection and electromagnetic compatibility increases significantly [1, 2].

The calculation of currents and voltages induced on a conductive object is performed using the integral equation of the electric field in the frequency domain [5, 6]. Initially, the currents are calculated at frequencies, and the temporal shape of the current pulses is obtained by the inverse Fourier transform for the convolution of the frequency representation of the currents with the spectrum

of the influencing pulse field [7].

Let us represent the total electric field as the sum of the incident field and the scattered field from the object under consideration $\vec{E}^i$ (fields without an object) and scattered $\vec{E}^s$ (fields induced by currents and charges on the object surface by the incident field) [8]:

$$\vec{E}(\vec{r},t) = \vec{E}(\vec{r}) \cdot \exp(j\omega t) = \vec{E}^i + \vec{E}^s, \quad (1)$$

where $\vec{r}$ is the position vector of the point in space; ω is the frequency of the incident field.

The scattered field is expressed through the currents $\vec{J}(\vec{r})$ and charges $\sigma(\vec{r})$ on the surface of the conductor S via the vector magnetic potential $\vec{A}(\vec{r})$ and scalar electric potential $\Phi(\vec{r})$ as follows (omitting the time dependence) [8]:

$$\vec{E}^s(\vec{r}) = -j\omega\vec{A}(\vec{r}) - \nabla\Phi(\vec{r}), \quad (2)$$

where

$$\vec{A}(\vec{r}) = \frac{\mu}{4\pi}\int_S \vec{J}(\vec{r}')\frac{\exp(-jkR)}{R}dS', \quad (3)$$

$$\Phi(\vec{r}) = \frac{1}{4\pi\varepsilon}\int_S \sigma(\vec{r}')\frac{\exp(-jkR)}{R}dS' = -\frac{1}{4\pi j\omega\varepsilon}\int_S \nabla_S\vec{J}(\vec{r}')\frac{\exp(-jkR)}{R}dS', \quad (4)$$

where k = 2π/λ is the wave number; $R = |\vec{r} - \vec{r}'|$ is the distance between an arbitrarily placed observation point $\vec{r}$ and the point of origin $\vec{r}'$ on the surface of the conductor S; μ, ε there are parameters of the surrounding environment; $\nabla_S\vec{J}$ is the surface divergence of the rotor $\vec{J}$.

After the transformations, we obtain an integral equation of the electric field:

$$\left(j\omega\vec{A}(\vec{r}) + \nabla\Phi(\vec{r})\right)_{\tan} = \vec{E}^i_{\tan} - Z_S\vec{J}(\vec{r}), \quad (5)$$

where $\vec{E}^i_{\tan}(\vec{r})$ is tangential to S (a component of the incident electric field).

For perfectly conducting objects, the integral equation of the electric field has a simpler form [7, 8]:

$$\left(j\omega\vec{A}(\vec{r}) + \nabla\Phi(\vec{r})\right)_{\tan} = \vec{E}^i_{\tan}. \quad (6)$$

Introducing the surface impedance allows the modeling of active and reactive resistance elements when solving scattering or radiation problems. For thin elongated conductors, the integral equation of the electric field is solved using the method of moments. In this case, the studied line is modeled by segments of a round wire, and the following approximations are made:

- the current flows only in the direction of the wire axis;
- the density of the current and charge is approximated by threads of current $\vec{I}$ and charge σ on the wire axis;
- the Leontovich boundary condition is applied only to the axial component of the field on the wire surface.

The schematic calculation of the current induced on an object by a pulsed electromagnetic field can be presented as shown in Fig. 1.

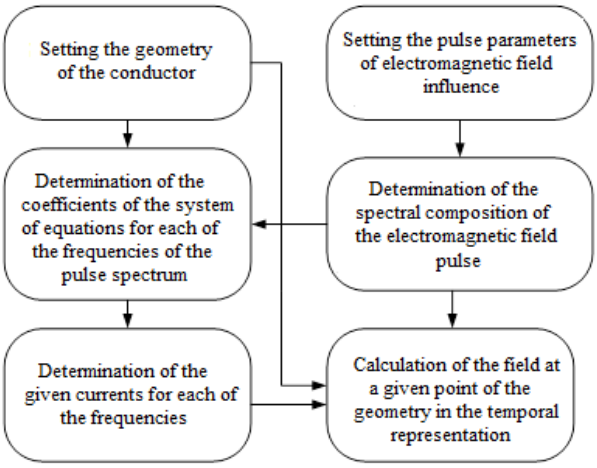

FIG. 1. Diagram of the calculation of the current induced on an object by a pulsed electromagnetic field.

In order to numerically solve the equation, the geometry of the object is approximated by straight wire segments. To each connection point of two wire segments (a non-boundary node), a basis function is assigned, which is non-zero only on the corresponding pair of segments, where it takes the form [3]:

$$\vec{f}_n(\vec{r}) = \frac{\pm(\vec{r}_n^{\pm} - \vec{r})}{l_n^{\pm}}. \quad (7)$$

where n is the node number; the signs «–» i «+» are assigned as indices to the first (W_n^-) and second (W_n^+) segments in the pair, respectively; $l_n^{\pm}$ is the length of the wired segment $W_n^{\pm}$; $\vec{r}_n^{\pm}$ is the position vector of the second (different from the n-th node) end of the wired segment $W_n^{\pm}$.

The effectiveness of the impact of ultra-wideband electromagnetic pulses largely depends on their wide bandwidth, which ensures the influence of electromagnetic radiation on various electronic equipment elements [9, 10].

The impact of ultra-wideband electromagnetic pulses on an object can be described using a transfer function [7]:

$$G = \frac{F_{out}(j\omega)}{F_{in}(j\omega)}, \quad (8)$$

where $F_{out}(j\omega)$ is the output function spectrum; $F_{in}(j\omega)$ is the impact spectrum.

The effectiveness of the impact can be determined as the ratio of energies [7]:

$$\eta_E = \frac{\int_0^{\infty}\left|F_{out}(j\omega)\right|^2 d\omega}{\int_0^{\infty}\left|F_{in}(j\omega)\right|^2 d\omega}. \quad (9)$$

So, the danger of the impact on protection systems and wearable IoT devices of a specific UWB electromagnetic pulse is determined not only by the amplitude, pulse front, and energy but also by the effectiveness of its impact on energy and voltage [9, 10].

III. EXPERIMENTAL RESEARCH

To experimentally determine the shielding coefficient of radio-opaque fabrics, an installation is proposed, the structural diagram of which is shown in Fig. 2.

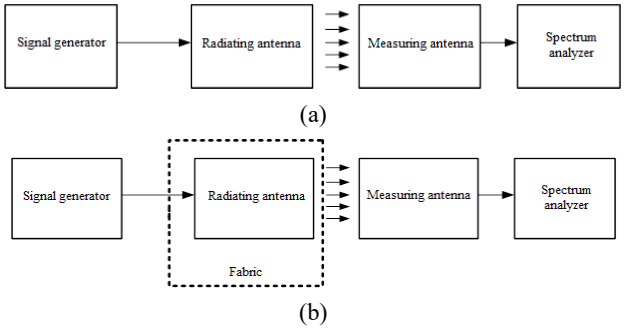

FIG. 2. Scheme for studying radio-opaque fabrics: (a) scheme for measuring electric field intensity without fabric; (b) scheme for measuring electric field intensity with fabric.

The setup consists of a signal generator, a transmitting antenna, a measuring antenna, and a spectrum analyzer. The signal generator, in combination with the transmitting antenna, is designed to create an electromagnetic field at the frequency being investigated. The measuring antenna in combination with the spectrum analyzer, is used to measure the intensity of the electromagnetic field at the location of the antenna at the established frequency. [6] The measuring antenna should be installed at a distance of at least 0.5 m from the transmitting antenna. To increase measurement accuracy, it is proposed to place the transmitting and measuring antennas in a separate room.

The measurements should be carried out in the following sequence. First, the intensity of the electric field of the transmitting antenna is measured in the range of the investigated frequencies according to the scheme shown in Fig. 2a. Then, the transmitting antenna is shielded by the fabric, and measurements are conducted according to the scheme shown in Fig. 2b. The investigation of radio-opaque fabrics G7 and G8 was conducted using the presented setup in the frequency range of 50 MHz ~ 2 GHz. The experimental results are presented in Table 1.

TABLE 1. Research Results of G7 and G8 Fabrics.

Frequency (MHz)	Fabric G7				Fabric G8			
	Transverse fiber orientation		Longitudinal fiber orientation		Transverse fiber orientation		Longitudinal fiber orientation	
	Shielding coefficient		Shielding coefficient		Shielding coefficient		Shielding coefficient	
	times	dB	times	dB	times	dB	times	dB
50	1,0	0,0	1,4	2,9	1,4	2,9	1	0,0
100	1,2	1,6	1,3	2,3	2,6	8,3	3,1	9,8
200	1,1	0,8	1,4	2,9	3,3	10,4	2,2	6,8
300	1,6	4,1	1,5	3,5	3,1	9,8	5,2	14,3
400	0,6	-5,0	1,1	0,8	4,4	12,9	6,2	15,8
500	1,8	5,1	2,3	7,2	4,1	12,3	4,7	13,4
600	2,0	6,0	1,8	5,1	5,2	14,3	7,1	17,0
700	2,2	6,8	2,1	6,4	4,8	13,6	5,3	14,5
800	2,1	6,4	1,7	4,6	3,6	11,1	4,2	12,5
900	2,5	8,0	1,9	5,6	4,3	12,7	2,8	8,9
1000	2,7	8,6	1,2	1,6	4,9	13,8	3,6	11,1
1100	3,3	10,4	3,2	10,1	6,4	16,1	8,4	18,5
1200	5,0	14,0	3,6	11,1	6,1	15,7	6,9	16,8
1300	4,3	12,7	3,1	9,8	11,4	21,1	7,8	17,8
1400	4,6	13,2	5,2	14,3	11,7	21,4	8,4	18,5
1500	6,1	15,7	6,3	16,0	12,2	21,7	6,7	16,5
1600	5,8	15,3	4,1	12,3	10,6	20,5	9,3	19,4
1700	7,2	17,1	5,1	14,2	11,1	20,9	7,7	17,7
1800	4,6	13,3	4,2	12,5	13,2	22,4	4,3	12,7
1900	3,9	11,8	2,2	6,8	11,4	21,1	6,3	16,0
2000	3,1	9,8	2,4	7,6	9,7	19,7	5,3	14,5

A programmable signal generator with a frequency range of 100 kHz ~ 2 GHz was used as a signal generator. The transmitting antenna, which was 20 cm long, was connected to it. The transmitting antenna was placed in rectangular dielectric housing. A dipole measuring antenna was used as the measuring antenna, which was

placed 1 m away from the transmitting antenna. The level of the measuring antenna signal was determined using a spectrum analyzer. The maximum error in this setup will be introduced by the measuring antenna, the error of which is ±2 dB. Therefore, we will consider the measurement error of the field intensity to be ±2 dB as well. After the measurements were taken, the shielding effectiveness of the electromagnetic field was determined.

Based on the discussed methodology, a study was conducted on the radio-opaque fabric G7 and fabric G8 in cases of longitudinal and transverse fiber placement. The research results are presented in Table 1.

Figure 3 shows the graphs of the shielding effectiveness as a function of frequency for the transverse and longitudinal orientations of Fabric G7 with respect to the polarization of the field, which visually represents the results presented in Table 1.

Figure 4 shows the graphs of the shielding effectiveness as a function of frequency for the transverse and longitudinal orientations of Fabric G8 with respect to the polarization of the field, which visually represents the results presented in Table 1.

The analysis of the graphs in Figure 3 shows that for the frequency range up to 1000 MHz, Fabric G7 has a low screening coefficient that varies within a range of 1 to 2.5 times.

At frequencies above 1000 MHz, the screening coefficient of the field increases. The screening coefficient increases to a maximum value of approximately 7.2 times at a frequency of 1700 MHz in the case of a transverse arrangement of fibers in the fabric with respect to the polarization of the field.

When the fibers are arranged longitudinally with respect to the polarization of the field, the screening coefficient behaves similarly to the case of transverse fiber arrangement. The maximum value of the screening coefficient is 6.3 times at a frequency of 1500 MHz.

The analysis of the graphs in Figure 4 shows that in the case of a transverse arrangement of fibers in Fabric G8, it has the highest screening coefficient in the frequency range of 1300-1900 MHz. In the case of a longitudinal arrangement of fibers in Fabric G8 with respect to the polarization of the field, the screening coefficient has a lower value, but its maximum value is observed with a step-like character in the frequency range of 1100-1700 MHz and is approximately 7 times.

Let us compare the radio-opaque fabrics G7 and G8 with each other. To compare, we present graphs of the dependence of the screening coefficient of fabrics G7 and G8 on one figure for cases of transverse (Figure 5) and longitudinal (Figure 6) arrangement of fibers in fabrics with respect to the polarization of the field.

Analysis of the graphs in Figure 5 shows that for the case of transverse fiber orientation, the frequencies at which the shielding coefficient reaches its maximum value differ slightly for the two fabrics. For Fabric G7, the shielding coefficient has a maximum at a frequency of 1700 MHz, while Fabric G8 has a maximum shielding coefficient at a frequency of 1800 MHz. The maximum shielding coefficient values for the two fabrics differ by a factor of two.

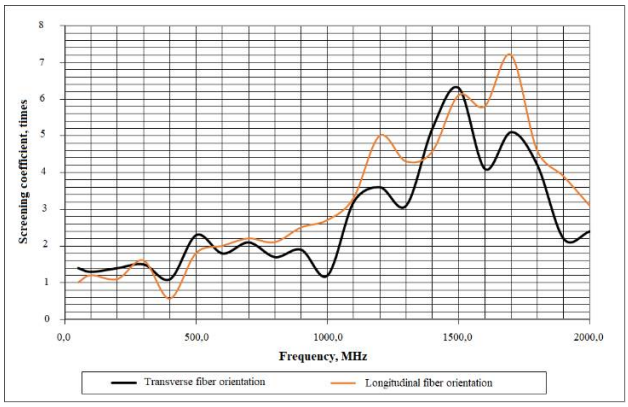

FIG. 3. Dependence of shielding effectiveness on frequency for G7 Fabric.

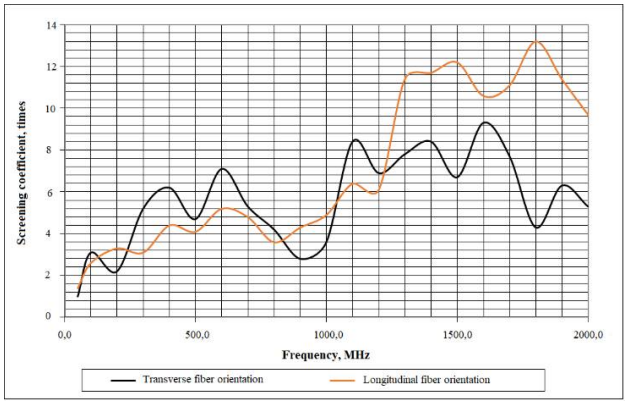

FIG. 4. Dependence of shielding effectiveness on frequency for G8 Fabric.

FIG. 5. Dependence of the screening coefficient on frequency for fabrics G7 and G8 in the case of transverse fiber orientation.

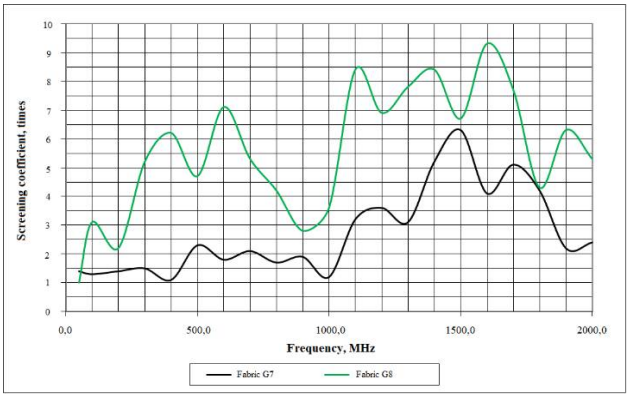

FIG. 6. Dependence of the shielding coefficient on frequency for fabrics G7 and G8 in the case of longitudinal fiber orientation.

Analysis of the graphs in Figure 6 shows that in the case of longitudinal fiber orientation relative to the polarization of the field, fabric G8 has two sub-ranges of maximum values, except for frequencies close to 900 MHz. Fabric G8 has a higher shielding effectiveness coefficient compared to fabric G7. The frequencies at which the shielding effectiveness coefficient reaches its maximum value are different for the two fabrics.

IV. CONCLUSION

Experimental studies were conducted on domestic radio-opaque fabrics G7 and G8 for the case of vertical and horizontal fiber orientation. The results showed that fabric G8 has better-shielding characteristics than fabric G7.

In the case of transverse fiber orientation, the shielding coefficient for Fabric G7 has a maximum at a frequency of 1700 MHz, while Fabric G8 has a maximum shielding coefficient at a frequency of 1800 MHz. The maximum shielding coefficient values for the two fabrics differ by a factor of two.

In the case of longitudinal fiber orientation, Fabric G8 has two sub-ranges of maximum shielding, except for frequencies close to 900 MHz. Fabric G8 has a higher shielding coefficient than Fabric G7. The frequencies at which the shielding coefficient reaches its maximum value differ for the two fabrics.

So, Fabric G8 has a shielding coefficient more than 5 times higher in a larger part of the investigated frequency range. Of course, this is not a large attenuation, but such fabrics can find their niche in the use of IoT systems.

AUTHOR CONTRIBUTIONS

M. P. – conceptualization, methodology; A. S.– investigation; O. S. – writing-original draft preparation; O. D. – writing-review and editing.

COMPETING INTERESTS

The authors declare the absence of competing interests.

REFERENCES

[1] Vineeta Shukla, “Review of electromagnetic interference shielding materials fabricated by iron ingredients,” Nanoscale Advances Journal, vol. 1, issue 5, pp. 1640-1671, 2019. DOI: 10.1039/C9NA00108E.

[2] S. Geetha, K.K. Satheesh Kumar, Chepuri R.K. Rao, M. Vijayan, and D.C. Trivedi, “EMI Shielding: Methods and Materials – A Review,” Journal of Applied Polymer Science, vol. 112, pp. 2073-2086, 2009. DOI: 10.1002/app.29812.

[3] Da-Eun Kwon, Dong-Hee Han, Kyung-Hwan Jung, Seung-Jae Lee, Jang-Oh Kim, and Cheol-Ha Baek, “Performance and feasibility evaluation for radiation shielding of metal oxides: Monte Carlo simulation,” Journal of the Korean Physical Society, vol. 82, pp. 813-817, February 2023. DOI: 10.1007/s40042-023-00744-7.

[4] J. Krishnasamy, A. Das, R. Alagirusamy, and G. Thilagavathi, “Textile fabrics and ferrite-loaded composite materials for electromagnetic-shielding applications,” Functional and Technical Textiles. Elsevier, pp. 313–332, 2023. DOI: 10.1016/b978-0-323-91593-9.00011-0.

[5] N. Aral, M. A. Duch, and M. Ardanuy, “Material characterization and Monte Carlo simulation of lead and non-lead X-Ray shielding materials,” Radiation Physics and Chemistry, vol. 174. Elsevier BV, p. 108892, Sep. 2020. DOI: 10.1016/j.radphyschem.2020.108892.

[6] T. Pušić, B. Šaravanja, and K. Malarić, “Electromagnetic Shielding Properties of Knitted Fabric Made from Polyamide Threads Coated with Silver,” Materials, vol. 14, no. 5. MDPI AG, p. 1281, Mar. 08, 2021. DOI: 10.3390/ma14051281.

[7] L. Cheng, T. Zhang, M. Guo, J. Li, S. Wang, and H. Tang, “Electromagnetic shielding effectiveness and mathematical model of stainless steel composite fabric,” The Journal of the Textile Institute, vol. 106, no. 6. Informa UK Limited, pp. 577–586, Jun. 23, 2014. DOI: 10.1080/00405000.2014.929275.

[8] M. J. Roeterink, D. G. Kelly, E. G. Dickson, M. T. Andrews, and E. C. Corcoran, “Analysis and Monte Carlo modelling of radio-opaque personal protective fabrics,” Journal of Radioanalytical and Nuclear Chemistry, vol. 300, no. 3. Springer Science and Business Media LLC, pp. 1131–1139, Feb. 27, 2014. DOI: 10.1007/s10967-014-3039-8.

[9] B. Mohamadzade, R. M. Hashmi, R. B. V. B. Simorangkir, R. Gharaei, S. Ur Rehman, and Q. H. Abbasi, “Recent Advances in Fabrication Methods for Flexible Antennas in Wearable Devices: State of the Art,” Sensors, vol. 19, no. 10. MDPI AG, p. 2312, May 19, 2019. DOI: 10.3390/s19102312.

[10] M. U. Ali Khan, R. Raad, F. Tubbal, P. I. Theoharis, S. Liu, and J. Foroughi, “Bending Analysis of Polymer-Based Flexible Antennas for Wearable, General IoT Applications: A Review,” Polymers, vol. 13, no. 3. MDPI AG, p. 357, Jan. 22, 2021. DOI: 10.3390/polym13030357.

Andriy Semenov

He received the Ph.D. degree from Vinnytsia National Technical University, Ukraine, in 2008 and received the Dr.Sc. degree from Lviv Polytechnic National University, Ukraine, in 2019. He is currently a Full Professor of Vinnytsia National Technical University. He has authored and co-authored over 350 scientific papers.

Maksym Prytula

He received the Ph.D. degree from Vinnytsia National Technical University, Ukraine, in 2021. He is currently an Associated Professor at Vinnytsia National Technical University. His areas of research interest include magnetic sensors and magnetic field measurements. He has over 35 scientific papers.

Oleksandr Stalchenko

He received the Ph.D. degree from Vinnytsia National Technical University, Ukraine, in 2015. He is currently an Associated Professor at Vinnytsia National Technical University. His areas of research interest include telecommunication networks. He has over 60 scientific papers.

Oleksandr Donskyi

He received master's degree from Vinnytsia National Technical University, Ukraine, in 2023. Now he is an entrant to a postgraduate course at the Vinnytsia National Technical University. The field of his interest is radio-frequency devices and means of communication.

Захист носимих пристроїв IoT від електромагнітного випромінювання з використанням екрануючих властивостей радіонепрозорих тканин

Андрій Семенов[1,*], Максим Притула[1], Олександр Стальченко[1] та Олександр Донський[1]

[1]Факультет інформаційних електронних систем, Вінницький національний технічний університет, Вінниця, Україна

*Автор-кореспондент (Електронна адреса: semenov.a.o@vntu.edu.ua)

АНОТАЦІЯ З кожним днем джерел електромагнітного випромінювання стає всі більше і більше. В більшості випадків, електромагнітне випромінювання негативно впливає на організм людини, тварин та інших живих істот, а також несприятливо впливає на роботу електронних приладів. Завдяки електромагнітному випромінюванню електронних приладів, з них може відбуватися витік інформації. Негативний вплив електромагнітного випромінювання на організм людини провокує високий рівень стомлюваності, головний і серцевий біль тощо. Повсякденне використання мобільної техніки, побутових магнітних електроприладів (наприклад, мікрохвильової печі), телекомунікаційних мереж ставить у зону ризику більшість населення планети. В іншому випадку, зовнішній вплив електромагнітних полів на різноманітні сенсори, які використовуються в IoT, може сприяти отриманню невірних даних із сенсорів. Потужний зовнішній вплив електромагнітного поля на пристрої, які проводять обробку великих масивів даних, може сприяти збою при математичних розрахунках. Таким чином, захист від електромагнітних полів потрібний не тільки для електронних пристроїв, але й і для захисту людини. Одним із сучасних матеріалів для захисту від електромагнітного випромінювання є радіонепрозорі тканини. Вони можуть використовуватись для захисту стаціонарних об'єктів і носимих пристроїв IoT та для захисту людини. В роботі були проаналізовані промислові екземпляри радіонепрозорих тканин іноземного та українського виробництва. Українські виробники продовжують розробляти нові варіанти радіонепрозорих тканин. Черговими варіантами радіонепрозорих тканин є тканини G7, G8 та G9. В статті була запропонована і описана методика дослідження екрануючих властивостей тканини. Були проведені експериментальні дослідження та розрахований коефіцієнт екранування в діапазоні частот 50 МГц – 2 ГГц для двох тканин G7 та G8. Експериментальні дослідження проводились для двох випадків розташування волокон тканини відносно випромінювальної антени та поляризації поля. Побудовані графіки залежностей коефіцієнта екранування для двох тканин при різних розташуваннях волокон тканин. Зроблено порівняльний аналіз коефіцієнтів затухання двох тканин між собою та зроблені відповідні висновки.

КЛЮЧОВІ СЛОВА Інтернет речей, радіонепрозорі тканини, коефіцієнт екранування, частота, електромагнітне поле.